

Jacqueline M. Cole,^{a,b*}
Michael C. W. Chan,^c Vernon C.
Gibson^d and Judith A. K.
Howard^e

^aCavendish Laboratory, University of Cambridge, J. J. Thomson Avenue, Cambridge CB3 0HE England, ^bDepartment of Chemistry, University of New Brunswick, PO Box 4400, Fredericton, New Brunswick E3B 5A3, Canada, ^cDepartment of Biology and Chemistry, City University of Hong Kong, Tat Chee Avenue, Kowloon Tong, Kowloon, Hong Kong, ^dDepartment of Chemistry, Imperial College London, Exhibition Road, London SW7 2AZ, England, and ^eDepartment of Chemistry, University of Durham, South Road, Durham DH1 3LE, England

Correspondence e-mail: jmc61@cam.ac.uk

Effects of the [OC₆F₅] moiety upon structural geometry: crystal structures of half-sandwich tantalum(V) aryloxy complexes from reaction of Cp^{*}Ta(N^tBu)(CH₂R)₂ with pentafluorophenol

Received 14 March 2011

Accepted 19 July 2011

The synthesis, chemical and structural characterization of a series of pentamethylcyclopentadienyl (Cp^{*}) tantalum imido complexes and aryloxy derivatives are presented. Specifically, the imido complexes Cp^{*}Ta(N^tBu)(CH₂R)₂, where R = Ph [dibenzyl(*tert*-butylamido) (η^5 -pentamethylcyclopentadienyl)tantalum(IV) (1)], Me₂Ph [*tert*-butylamido)bis(2-methyl-2-phenylpropyl) (η^5 -pentamethylcyclopentadienyl)tantalum(IV) (2)], CMe₃ [(*tert*-butylamido)bis(2,2-dimethylpropyl) (η^5 -pentamethylcyclopentadienyl)tantalum(IV) (3)], are reported. The crystal structure of (3) reveals α -agostic interactions with the Ta atom. The resulting increase in the tantalum core coordination improves electronic stability. As such it does not react with pentafluorophenol, in contrast to the other two reported imido complexes [(1) and (2)]. Addition of C₆F₅OH to (1) yields a dimeric aryl-oxide derivative, [Cp^{*}Ta(CH₂Ph)(OC₆H₅)(μ -O)]₂ [di- μ -oxido-bis[benzyl(pentafluorophenolato) (η^5 -pentamethylcyclopentadienyl)tantalum(V)] (4)]. Its crystal structure reveals long Ta—O(C₆H₅) bonds but short oxo-bridging Ta—O bonds. This is explained by accounting for the fierce electronic competition for the vacant d_{π} orbitals of the electrophilic Ta^V centre. Steric congestion around each metal is alleviated by a large twist angle (77.1°) between the benzyl and pentafluorophenyl ligands and the ordering of each of these groups into stacked pairs. The imido complex (2) reacts with C₆F₅OH to produce a mixture of Cp^{*}Ta(OC₆F₅)₄ [tetrakis(pentafluorophenolato)-(η^5 -pentamethylcyclopentadienyl)tantalum(V) (5)] and [Cp^{*}Ta(OC₆F₅)₂(μ -O)]₂ [di- μ -oxido-bis[bis(pentafluorophenolato)(η^5 -pentamethylcyclopentadienyl)tantalum(V)] (6)]. Steric congestion is offset in both cases by the twisting of its pentafluorophenyl ligands. Particularly strong electronic competition for the empty d_{π} metal orbitals in (6) is reflected in its bond geometry, and owes itself to the more numerous electron-withdrawing pentafluorophenyl ligands. The balance of steric and electronic factors affecting the reactivity of Cp^{*}tantalum imido based complexes with pentafluorophenol is therefore addressed.

1. Introduction

High-oxidation transition-metal complexes have found widespread application as reagents in organic synthesis (Negishi, 1991; Buchwald & Nielsen, 1988; Schwartz & Labinger, 1976, and references therein; Takahashi *et al.*, 1991; Tidwell *et al.*, 1991) and as polymerization catalysts (Coles *et al.*, 1995; Schoettel *et al.*, 1989; Jordan, 1991; Kaminsky, 1994; Tilley, 1993). Such compounds containing a transition metal of a low d^n configuration have shown particular promise since in these complexes the metal environment is electron deficient. As a result there has been much interest in Group IVA complexes

(Coles *et al.*, 1995; Jordan, 1991; Kaminsky, 1994; Tilley, 1993; Brintzinger *et al.*, 1995) and especially in bent metallocene complexes (Jordan *et al.*, 1986; Hlatky *et al.*, 1989; Ewen & Elder, 1993; Chien *et al.*, 1991; Yang *et al.*, 1991, 1994; Buchwald *et al.*, 1986, 1989).

Group VA complexes are of interest since they are isolobal to Group IVA bent metallocene complexes. In this regard, each cyclopentadienyl (Cp) ligand is isolobal with a ligand of the general formula, RN^{2-} and RO^- . Oxo ligands have been found to stabilize high-oxidation transition-metal complexes due to their ability to participate in extensive ligand-to-metal π donation (Nugent & Mayer, 1988). This motivated the synthesis and characterization of a series of half-sandwich tantalum aryloxy Group VA complexes. Specifically, the formation of a series of pentamethyl-cyclopentadienyl tantalum imido complexes and their subsequent reactions with pentafluorophenol were investigated. An overview of the reactions involved is illustrated in Fig. 1.

2. Experimental

2.1. Synthesis and chemical characterization

All manipulations were performed under an atmosphere of nitrogen using standard Schlenk and cannular techniques or in a conventional nitrogen-filled glove-box. Solvents were refluxed over a suitable drying agent and distilled and degassed prior to use. Elemental analyses were performed by the microanalytical services of the Department of Chemistry, Durham University. IR spectra (Nujol mulls, CsI windows) were recorded on Perkin–Elmer 577 and 457 grating spectrophotometers, mass spectra on a VG 7070E Organic Mass Spectrometer, and NMR spectra on a Varian VXR 400S spectrometer for 1H (400.0 MHz), ^{13}C (100.6 MHz) and ^{19}F (376.3 MHz) nuclei in C_6D_6 (chemical shifts are referenced to the residual protio impurity). Expected coupling constants are omitted. $Cp^*Ta(N^iBu)Cl_2$ was prepared by a literature method (Schmidt & Sundermeyer, 1994). All other chemicals were

obtained commercially and used as received unless stated otherwise.

2.1.1. $Cp^*Ta(N^iBu)(CH_2Ph)_2$ (1). Benzylmagnesium chloride (1.0 M in Et_2O , 4.09 ml, 4.09 mmol) was added to a stirred solution of $Cp^*Ta(N^iBu)Cl_2$ (0.89 g, 1.95 mmol) in diethyl ether (50 ml) at 195 K. The mixture was allowed to warm up to room temperature to give a yellow solution and white precipitate. After 10 h all volatile components were removed under reduced pressure to leave a yellow solid. Extraction with pentane followed by removal of solvent *in vacuo* afforded a bright yellow solid. Yield 0.89 g, 88%; found: C 58.6, H 6.9, N 2.5%; $C_{28}H_{38}NTa$ requires: C 59.05, H 6.7, N 2.5%; ν_{max} (cm^{-1}): 1595, 1485, 1350, 1265, 1205, 800, 745, 695; m/z 570 (M^+); NMR: 1H , δ 1.09 (s, 9H, CMe_3), 1.38 (d, 2H, $^2J_{HH} = 12.0$ Hz, CH_2Ph), 1.77 (s, 15H, C_5Me_5), 2.07 (d, 2H, $^2J_{HH} = 12.0$ Hz, CH_2Ph), 6.93 (t, 2H, *p*-Ph), 7.05 (d, 4H, *o*-Ph), 7.20 (t, 4H, *m*-Ph); ^{13}C , δ 11.4 (q, C_5Me_5), 33.2 (q, CMe_3), 65.2 (s, CMe_3), 71.3 (t, $^1J_{CH} = 119$ Hz, CH_2Ph), 115.9 (s, C_5Me_5), 122.8 (d, *p*-Ph), 128.1 (d, *m*-Ph), 128.9 (d, *o*-Ph), 149.4 (s, *ipso*-Ph).

2.1.2. $Cp^*Ta(N^iBu)(CH_2CMe_2Ph)_2$ (2). Neophylmagnesium chloride (1.29 M in Et_2O , 1.35 ml, 1.74 mmol) was added to a solution of $Cp^*Ta(N^iBu)Cl_2$ (0.38 g, 0.83 mmol) in diethyl ether (40 ml) at 195 K. The mixture was allowed to warm up to room temperature and stirred for 18 h to give a dark yellow solution and white precipitate. All volatile components were removed under reduced pressure and extraction with pentane followed by removal of solvent *in vacuo* afforded a brown oily solid. Recrystallization in acetonitrile at 273 K yielded yellow crystals. Yield 0.28 g, 52%; found: C 62.6, H 7.8, N 2.4%; $C_{34}H_{50}NTa$ requires C 62.5, H 7.7, N 2.1%; ν_{max} (cm^{-1}): 1990, 1495, 1355, 1255, 1030, 765, 695; m/z 654 (M^+); NMR: 1H , δ -0.42 (d, 2H, $^2J_{HH} = 13.0$ Hz, CH_2), 1.46 (s, 9H, CMe_3), 1.58 (d, 2H, $^2J_{HH} = 13.0$ Hz, CH_2), 1.62 (s, 6H, CMe_2Ph), 1.70 (s, 15H, C_5Me_5), 1.79 (s, 6H, CMe_2Ph), 7.09 (t, 2H, *p*-Ph), 7.24 (t, 4H, *m*-Ph), 7.43 (d, 4H, *o*-Ph); ^{13}C , δ 11.6 (q, C_5Me_5), 33.9 (q, CMe_2Ph), 34.1 (q, CMe_3), 35.2 (q, CMe_2Ph), 41.5 (s, CMe_2Ph), 65.4 (s, CMe_3), 91.5 (t, $^1J_{CH} = 109$ Hz, CH_2), 115.6 (s, C_5Me_5), 125.2 (d, *p*-Ph), 126.0 (d, *m*-Ph), 128.2 (d, *o*-Ph), 155.3 (s, *ipso*-Ph).

2.1.3. $Cp^*Ta(N^iBu)(CH_2CMe_3)_2$ (3). Neopentylmagnesium chloride (0.82 M in Et_2O , 4.98 ml, 4.09 mmol) was added to a solution of $Cp^*Ta(N^iBu)Cl_2$ (0.85 g, 1.86 mmol) in diethyl ether (60 ml) at 195 K. The mixture was allowed to warm up to room temperature and stirred for 12 h. The resultant yellow solution was filtered from the white precipitate and all volatile components were removed under reduced pressure to give a yellow solid. Extraction with pentane followed by recrystallization in acetonitrile at 253 K yielded yellow crystals. Yield 0.87 g, 88%; found: C 54.3, H 8.9, N 2.7%; $C_{24}H_{46}NTa$ requires C 54.4, H 8.8, N 2.6%; ν_{max} (cm^{-1}): 1355, 1255, 1210, 805, 755, 535; m/z 529 (M^+); NMR: 1H , δ -0.61 (d, 2H, $^2J_{HH} = 12.8$ Hz, CH_2), 1.35 (s, 18H, CH_2CMe_3), 1.39 (d, 2H, $^2J_{HH} = 12.8$ Hz, CH_2), 1.51 (s, 9H, $NCMe_3$), 1.79 (s, 15H, C_5Me_5); ^{13}C , δ 11.7 (q, C_5Me_5), 34.3 (q, $NCMe_3$), 34.8 (s, CH_2CMe_3), 35.6 (q, CH_2CMe_3), 65.3 (s, $NCMe_3$), 90.4 (t, $^1J_{CH} = 106$ Hz, CH_2), 115.3 (s, C_5Me_5).

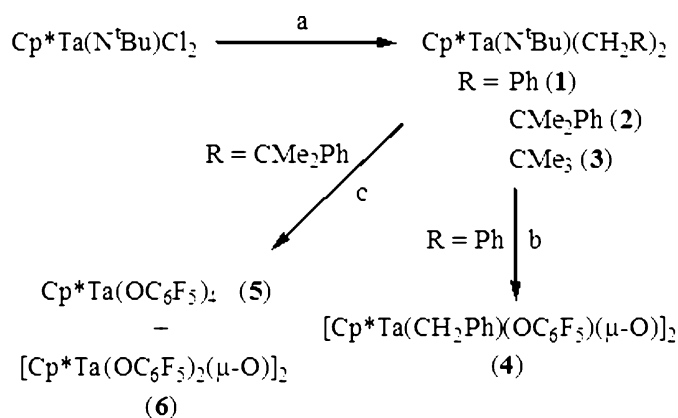


Figure 1

A summary of the chemical formation of $Cp^*Ta(N^iBu)(CH_2R)_2$ and its subsequent reactivity with pentafluorophenol: (a) 2 RC_6H_5MgCl , Et_2O ; (b) 2 C_6F_5OH , toluene; (c) 2 C_6F_5OH , toluene, 333 K for 10 d.

Table 1

Experimental details.

Experiments were carried out at 150 K with Mo $K\alpha$ radiation. Empirical absorption corrections were applied.

	(3)	(4)	(5)	(6)
Crystal data				
Chemical formula	C ₂₄ H ₄₆ N ₂ Ta	C ₂₃ H ₂₂ F ₅ O ₂ Ta	C ₃₄ H ₁₅ F ₂₀ O ₄ Ta	C ₄₄ H ₃₀ F ₂₀ O ₆ Ta ₂ ·C ₇ H ₈
M_r	529.57	606.36	1048.41	1488.71
Crystal system, space group	Monoclinic, $P2_1/c$	Triclinic, $P\bar{1}$	Orthorhombic, $Pbcm$	Monoclinic, $P2_1/n$
a, b, c (Å)	9.083 (2), 16.216 (3), 16.872 (3)	9.239 (2), 11.647 (2), 11.803 (2)	8.341 (2), 26.389 (5), 15.145 (3)	12.793 (2), 15.242 (2), 25.708 (3)
α, β, γ (°)	90, 99.76 (3), 90	117.25 (3), 96.37 (3), 106.63 (3)	90, 90, 90	90, 100.178 (5), 90
V (Å ³)	2449.1 (8)	1037.3 (3)	3333.6 (12)	4933.9 (12)
Z	4	2	4	4
μ (mm ⁻¹)	4.50	5.36	3.45	4.56
Crystal size (mm)	0.26 × 0.24 × 0.20	0.80 × 0.64 × 0.44	0.46 × 0.12 × 0.08	0.8 × 0.45 × 0.3
Data collection				
Diffractometer	Siemens P4	Siemens P4	Siemens P4	Siemens SMART CCD
T_{\min} , T_{\max}	0.267, 0.365	0.261, 1.000	0.674, 0.770	0.343, 0.447
No. of measured, independent and observed [$I > 2\sigma(I)$] reflections	13 104, 10 777, 7822	3942, 3310, 2985	3749, 3043, 2150	17 825, 6926, 6101
R_{int}	0.030	0.145	0.054	0.053
θ_{max} (°)	35.0	25.0	25.0	23.3
Refinement				
$R[F^2 > 2\sigma(F^2)]$, $wR(F^2)$, S	0.038, 0.064, 1.03	0.073, 0.182, 1.02	0.045, 0.101, 1.01	0.063, 0.094, 2.26
No. of reflections	10 774	3309	3043	6922
No. of parameters	247	221	283	619
H-atom treatment	H atoms treated by a mixture of independent and constrained refinement	H atoms treated by a mixture of independent and constrained refinement	Riding†	Riding†
$\Delta\rho_{\text{max}}$, $\Delta\rho_{\text{min}}$ (e Å ⁻³)	1.10, -0.79	5.30, -3.77	0.85, -1.09	1.32, -0.96

† H atoms treated by the riding model $U_{\text{iso}}(\text{H}) = 1.2U_{\text{eq}}(\text{C})$, except where they belong to a methyl group, in which case $U_{\text{iso}}(\text{H}) = 1.5U_{\text{eq}}(\text{C})$.

2.1.4. [Cp*Ta(CH₂Ph)(OC₆F₅)(μ-O)]₂ (4). C₆F₅OH (0.32 g, 1.74 mmol) in cold toluene (20 ml at 195 K) was added dropwise to a stirred solution of Cp*Ta(N^tBu)(CH₂Ph)₂ (1) (0.50 g, 0.87 mmol) in cold toluene (40 ml) at 195 K. The mixture was allowed to warm up to room temperature over 90 min to afford a bright red solution. After stirring for a further 12 h, the solution was filtered, concentrated and cooled to 243 K to give bright yellow hexagonal crystals. Yield 0.23 g, 22%; found: C 45.4, H 3.9%; C₄₆H₄₄O₄F₁₀Ta₂ requires C 45.6, H 3.7%; ν_{max} (cm⁻¹) 1505, 1315, 1260, 1190, 1165, 985, 800, 755, 700; NMR: ¹H, δ 1.58 (s, 15H, C₅Me₅), 2.80 and 2.97 (dd, 2H, ²J_{HH} = 13.6 Hz, CH₂Ph), 7.03 (t, 1H, *p*-Ph), 7.16 (d, 2H, *o*-Ph), 7.39 (t, 2H, *m*-Ph); ¹³C (decoupled), δ 10.4 (C₅Me₅), 73.1 (CH₂Ph), C₅Me₅ not resolved, 123.1, 127.5, 131.2 (*o*-, *m*- and *p*-Ph), 132–142 (C₆F₅), 143.9 (*ipso*-Ph); ¹⁹F, δ -157.5 (d, 2F, *o*-C₆F₅), -166.9 (t, 2F, *m*-C₆F₅), -172.5 (t, 1F, *p*-C₆F₅).

2.1.5. Cp*Ta(OC₆F₅)₄ (5) and [Cp*Ta(OC₆F₅)₂(μ-O)]₂ (6). C₆F₅OH (0.25 g, 1.34 mmol) in heptane (30 ml) was added dropwise to a solution of Cp*Ta(N^tBu)(CH₂CMe₂Ph)₂ (2) (0.44 g, 0.67 mmol) in cold heptane (50 ml) at 195 K. The mixture was allowed to warm up to room temperature and was then heated to 333 K. After stirring for 10 d, pale yellow needle-shaped crystals of pure (5) formed on the side of the vessel (yield 0.14 g, 20%). The filtrate was collected, concentrated and cooled to 253 K to give yellow needles of a mixture of (5) and (6). Repeated recrystallizations in toluene to

separate the two products eventually afforded pure (6) (yield 0.11 g, 12%). Complex (5): found: C 39.1, H 1.6%; C₃₄H₁₅O₄F₂₀Ta requires C 38.95, H 1.4%; m/z 864 (M^+ - OC₆F₅); NMR: ¹H, δ 2.04 (s); ¹³C, δ 10.7 (q, C₅Me₅), 109.5 (s, C₅Me₅), 134–141 (C₆F₅); ¹⁹F, δ -159.5 (d, 2F, *o*-C₆F₅), -164.6 (t, 2F, *m*-C₆F₅), -166.7 (t, 1F, *p*-C₆F₅). Complex (6): found: C 38.1, H 2.5%; C₄₄H₃₀O₆F₂₀Ta₂ requires C 37.8, H 2.2%; NMR: ¹H, δ 1.71 (s); ¹³C, δ 10.2 (q, C₅Me₅), 134–141 (C₆F₅), C₅Me₅ not resolved; ¹⁹F, δ -157.4 (d, 2F, *o*-C₆F₅), -165.6 (t, 2F, *m*-C₆F₅), -169.7 (t, 1F, *p*-C₆F₅).

2.2. Single-crystal X-ray diffraction analysis

All crystals were mounted onto a diffractometer using the oil-drop method (Kottke & Stalke, 1993). Single-crystal X-ray diffraction data for (3), (4) and (5) were collected using the Siemens P4 diffractometer whilst data for (6) were obtained using the Siemens SMART-CCD diffractometer. Graphite-monochromated Mo $K\alpha$ radiation ($\lambda = 0.71073$ Å) was used throughout. Data collections were carried out at 150 K and no decay was observed during any of the experiments. For (3), (4) and (5), cell refinement, data collection and data reduction proceeded *via* Siemens XSCANS (Siemens Analytical X-ray Instruments, 1994), whereas Siemens SMART software (Siemens Analytical X-ray Instruments, 1995a,b) was used to process data for (6). All crystal structures were solved using

SHELXS86 (Sheldrick, 2008) by Patterson and difference-Fourier methods. An absorption correction was applied to each data set: semi-empirical corrections using φ scans were applied in *XPREF* (Sheldrick, 2008) for (3), (4) and (5), whilst *DIFABS* (Walker & Stuart, 1983) was used to correct the data for (6). Subsequent least-squares refinement used the *SHELXL93* (Sheldrick, 2008) package. Scattering factors were taken from *International Tables for Crystallography* (1992, Vol. C, Tables 4.2.6.8 and 6.1.1.4). All non-H positional parameters were refined as were the hydrogen positions of (3) and (5). Anisotropic displacement parameters were refined for all non-H atoms except for the C atoms, C14–C18A of the Cp* ring in (4), and C30–C34B of the Cp* ring and C35–C41 of the toluene solvent in (6). Molecular disorder in the Cp* ring of (6) was modelled according to a split in each methyl group with 2:1 occupancy. The final residual electron-density map indicates that the main Cp* ring could also exhibit a small amount of disorder, in the form of a staggered conformation about C30–C34. However, the associated residual electron density is of the same order as the experimental noise ($\sim 1 \text{ e } \text{Å}^{-3}$) and all attempts to model this as a disordered feature resulted in zero occupancy and an unstable refinement. All H atoms were located geometrically except those adjoining C bridging atoms, *i.e.* H11A, H11B, H16A and H16B in (3) and H7A and H7B in (4). Isotropic displacement parameters of all H atoms were modelled in the riding model [$U_{\text{iso}}(\text{H}) = 1.2 U_{\text{eq}}(\text{C})$], except where they belonged to a methyl group, in which case $U_{\text{iso}}(\text{H}) = 1.5 U_{\text{eq}}(\text{C})$. A summary of crystal, data collection and refinement parameters for the structural determinations of (3), (4), (5) and (6) is given in Table 1.

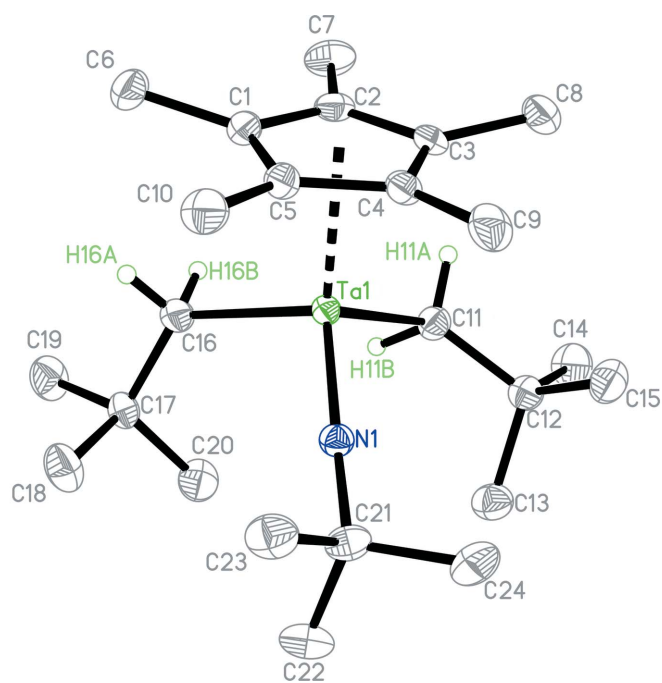


Figure 2

The molecular structure of (3) with anisotropic displacement parameters shown at the 50% probability level. H atoms are omitted for clarity except for those that adjoin the carbon bridging atoms.

Table 2

Selected bond lengths (Å) and angles (°) for (3).

Ta1–N1	1.788 (2)	N1–Ta1–C11	103.6 (1)
Ta1–C1	2.527 (3)	N1–Ta1–C16	105.0 (1)
Ta1–C2	2.554 (3)	N1–Ta1–Cp _{centroid}	126.1 (2)
Ta1–C3	2.504 (3)	C11–Ta1–C16	101.8 (1)
Ta1–C4	2.425 (3)	C11–Ta1–Cp _{centroid}	110.3 (2)
Ta1–C5	2.429 (3)	C16–Ta1–Cp _{centroid}	107.4 (3)
Ta1–Cp _{centroid}	2.175 (3)	Ta1–N1–C21	170.7 (2)
Ta1–C11	2.199 (3)	Ta1–C11–C12	128.8 (2)
Ta1–C16	2.208 (3)	Ta1–C11–H11a	108 (2)
C11–H11a	0.99 (4)	Ta1–C11–H11b	89 (2)
C11–H11b	1.01 (4)	Ta1–C16–C17	126.7 (2)
C16–H16a	0.91 (4)	Ta1–C16–H16a	111 (2)
C16–H16b	1.01 (4)	Ta1–C16–H16b	99 (2)
Ta1...H11b	2.40 (4)	Ta1...H11b–C11	66.1 (9)
Ta1...H16b	2.57 (4)	Ta1...H16b–C16	58.0 (9)

3. Results and discussion

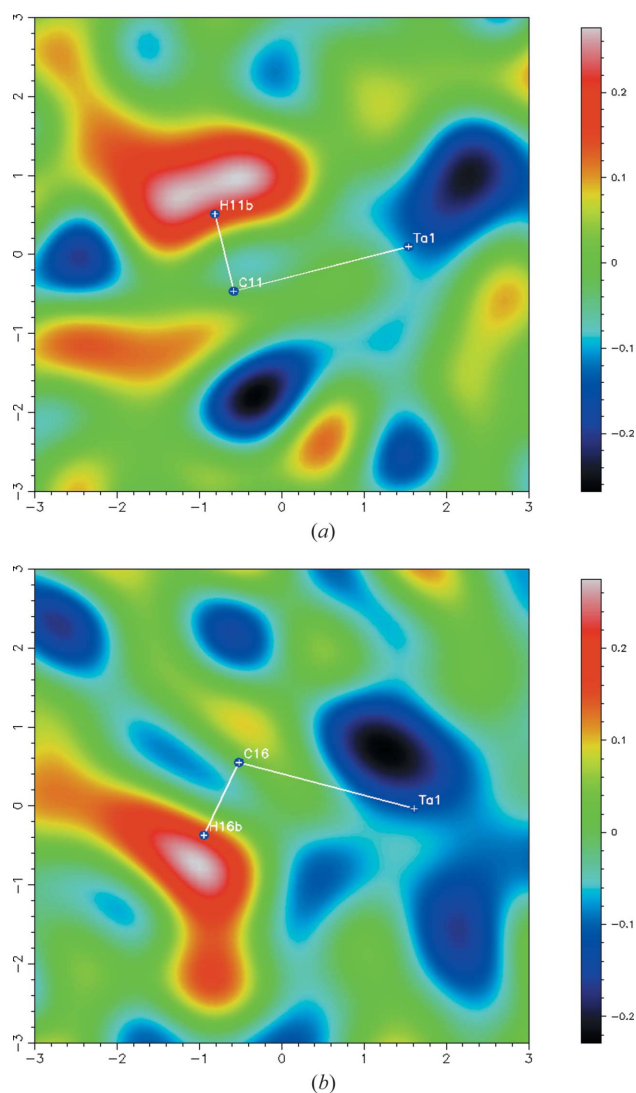
3.1. Crystal structure of (3) revealing α -agostic interactions

Treatment of $[\text{Cp}^*\text{Ta}(\text{N}^i\text{Bu})\text{Cl}_2]$ with 2 equiv. of the appropriate Grignard reagent RCH_2MgCl in diethyl ether readily affords the dialkyl complexes $[\text{Cp}^*\text{Ta}(\text{N}^i\text{Bu})(\text{CH}_2\text{R})_2]$ [$\text{R} = \text{Ph}$ (1), CMe_2Ph (2), CMe_3 (3)]. The low $^1J_{\text{CH}}$ coupling constant (106 Hz) of the metal-bound methylene groups in (3) is indicative of the presence of weak α -agostic interactions (Poole *et al.*, 1993) and this is supported herein by an X-ray structural determination (Fig. 2). Selected bond distances and angles for (3) are given in Table 2. Fractional coordinates and anisotropic displacement parameters are provided in the supplementary material.¹

The Ta atom lies in a pseudo-tetrahedral environment. The Ta1–N1 bond length [1.788 (2) Å] is within the expected range for a tantalum imido complex (Nugent & Harlow, 1978; Chamberlain *et al.*, 1986) and the imido angle Ta1–N1–C21 is close to linearity [170.7 (2)°]. A bulky Cp* group expectedly causes slight distortion from ideal tetrahedral geometry. Meanwhile, two neopentyl methylene groups comprise the other two ligands. This ostensibly four-coordinate Ta centre is suspicious given that tantalum typically accommodates higher coordination; indeed there are only two other recorded four-coordinate tantalum imido complexes that contain a CH_2CMe_3 ligand, the most relevant being [(2,6-diisopropylphenylimido)TaCp*H(CH₂CMe₃)] due to its Cp* substituent (Burckhardt *et al.*, 2002). There the Ta–C bond length is 2.121 (7) Å which is significantly shorter than the analogous Ta–C11 [2.199 (3) Å] and Ta–C16 [2.208 (3) Å] bond distances in this study. The Ta–C(CH₂CMe₃) bond lengths in (3) are, in fact, more statistically aligned with a coordination number of (5) or (6), *cf.* five-coordinate: $\bar{x} = 2.190$ (6) Å from $N = 24$ observations; six-coordinate: $\bar{x} = 2.238$ (7) Å, $N_{\text{obs}} = 29$ (ConQuest, Version 1.12; Bruno *et al.*, 2002; CCDC, 1994).

The presence of α -agostic interactions would augment the tantalum coordination number to a level commensurate with these statistics. With observations from ^1H NMR spectroscopy

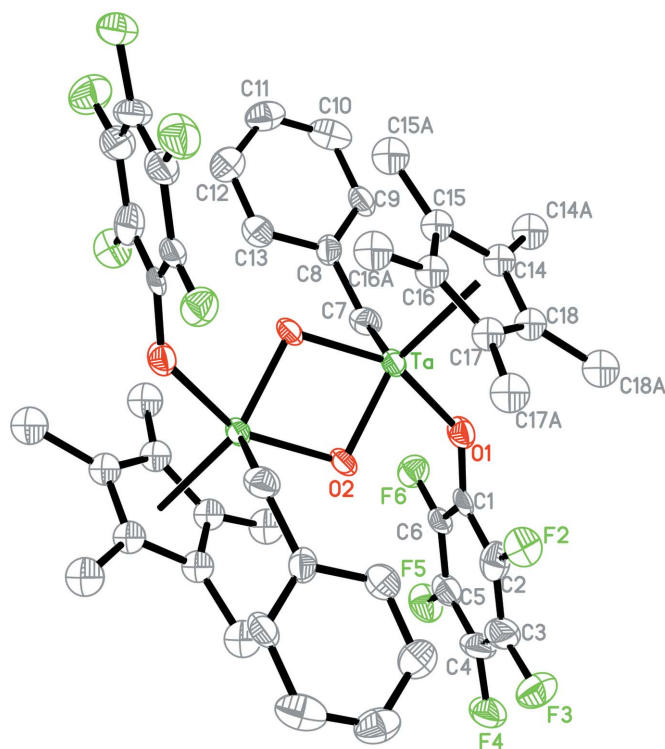
¹ Supplementary data for this paper are available from the IUCr electronic archives (Reference: ZB5019). Services for accessing these data are described at the back of the journal.


Figure 3

Fourier-difference electron density maps (in $e \text{ \AA}^{-3}$) showing planes in (3) that are defined by Ta, $C_{\text{methylene}}$ and the peak of maximum residual electron density (assigned to H; red/white) that lies in the vicinity of each $C_{\text{methylene}}$ and corresponds to a reasonable C–H bond length. This figure is in colour in the electronic version of this paper.

indicating that such interactions may be present, this X-ray diffraction study was undertaken at higher resolution ($d_{\text{min}} = 0.62 \text{ \AA}$) than is conventional ($d_{\text{min}} = 0.84 \text{ \AA}$). Having modelled all non-H atoms, the residual electron density around the tantalum and methylene groups was investigated (see Fig. 3). Unmodelled electron density is readily observable at approximately 1 \AA from each carbon, *i.e.* reminiscent of a C–H bond length.² The C–H vectors are distinctly oriented towards the Ta centre [Ta1–C11–H11b: $89(2)^\circ$; Ta1–C16–H16b: $99(2)^\circ$], with each H atom lying in close contact with the metal [Ta1 \cdots H11b $2.40(4)$, Ta1 \cdots H16b $2.57(4) \text{ \AA}$]. These bond-geometry considerations classify them as α -agostic interactions; see, for example, α -agostic interactions in the related complex [CpNb(N-2,6-*i*-Pr₂C₆H₃)(CH₂CMe₃)₂]

² All methylene H atoms (H11a, H11b, H16a and H16b) were found explicitly in the Fourier difference map and their positions were freely refined.


Figure 4

The molecular structure of (4) with anisotropic displacement parameters shown at the 50% probability level. H atoms are omitted for clarity. Only atoms in the asymmetric unit are labelled; the other half is related by an inversion centre.

(Nb \cdots H $_{\alpha}$ mean 2.36 \AA , Nb–C $_{\alpha}$ –H $_{\alpha}$ 87 and 89° ; Poole *et al.*, 1993) and the isolobal [Mo(N-2,6-*i*-Pr₂C₆H₃)(N^{*t*}Bu)(CH₂CMe₃)₂] (Mo \cdots H $_{\alpha}$ mean 2.40 \AA , Mo–C $_{\alpha}$ –H $_{\alpha}$ 91 and 98° ; Bell *et al.*, 1994). In addition, the orientation of both neopentyl groups towards the imido moiety, which would be sterically disfavoured, implies an electronic preference for this configuration due to the agostic interactions.

3.2. Chemical products from reaction of (1)–(3) with pentafluorophenol

3.2.1. Crystal structure of (4). Treatment of (1) with two molar equivalents of C₆F₅OH in toluene gives a bright red solution from which yellow crystals are obtained. Analysis by ¹H NMR spectroscopy indicates the presence of Cp* and benzyl groups in a 1:1 ratio, while ¹⁹F NMR data support the expected ligation of the [OC₆F₅] moiety. Elemental analysis confirms the removal of the *t*-butylimido substituent. The product is shown by X-ray crystallography to be the tantalum(V) dimer [Cp*Ta(CH₂Ph)(OC₆F₅)(μ -O)]₂ (4). Its formation is likely to proceed *via* the initial protonation and elimination of the imido moiety as *t*-butylamine³ to form the bis(aryloxo) intermediate [Cp*Ta(CH₂Ph)₂(OC₆F₅)₂]. The presence of an oxo bridge is unexpected and presumably results from the loss of bis(pentafluorophenyl) ether.

³ ¹H NMR monitoring of the reaction in C₆D₆ shows the appearance of butylamine before resonances for toluene are observed, hence this suggests that the imido group is protonated before the benzyl ligand.

Table 3

Selected bond lengths (Å) and angles (°) for (4).

Ta—O1	2.005 (8)	O1—Ta—O2	80.7 (3)
Ta—O2	1.957 (7)	O1—Ta—O2#1	150.8 (4)
Ta—O2#1	1.950 (8)	O1—Ta—C7	83.2 (4)
Ta—C7	2.20 (1)	O1—Ta—Cp _{centroid}	102.2 (4)
Ta—C14	2.56 (1)	O2—Ta—O2#1	76.7 (3)
Ta—C15	2.53 (1)	O2—Ta—C7	113.4 (4)
Ta—C16	2.45 (1)	O2—Ta—Cp _{centroid}	137.6 (4)
Ta—C17	2.39 (1)	O2#1—Ta—C7	89.1 (4)
Ta—C18	2.48 (2)	O2#1—Ta—Cp _{centroid}	106.9 (4)
Ta—Cp _{centroid}	2.17 (3)	C7—Ta—Cp _{centroid}	108.9 (5)
		Ta—O1—C1	139.8 (8)
		Ta—O2—Ta#1	103.3 (3)
		Ta—C7—C8	125.2 (8)

The molecular structure of (4) is shown in Fig. 4, and selected bond distances and angles are given in Table 3. Fractional coordinates and anisotropic displacement parameters are given in the supplementary material.

Complex (4) is a centrosymmetric oxo-bridged dimer with the Ta atom adopting a distorted square-pyramidal configuration. The aryloxo Ta—O1 bond length of 2.005 (8) Å is noteworthy since it corresponds to the upper quartile of all known Ta^V—OC_{aryl} distances (*ConQuest*, Version 1.12; Bruno *et al.*, 2002; CCDC, 1994), *cf.* UQ = 2.01 Å in the skewed distribution of $N = 542$ observations; range 1.77–2.32 (7) Å; skew = 2.08. In stark contrast the bridged oxo Ta—O2 bonds are markedly short [1.957 (7) and 1.950 (8) Å], given a statistical analysis of all reported TaO distances in Ta(O₂)Ta bridging crystal structures, *cf.* $\bar{x} = 2.118$ (9) Å, in the range 1.944–2.403 Å from $N = 105$ observations (Bruno *et al.*, 2002; CCDC, 1994); indeed, only two observations have shorter Ta—O bond lengths (Abbenhies *et al.*, 1992; Abrahams *et al.*, 2000). These Ta—O bond-length observations can be rationalized by considering the fierce competition for the vacant d_{π} symmetry orbitals of the electrophilic Ta^V centre. There are three O atoms per metal attempting to participate in p_{π} – d_{π} interactions *via* donation from their lone pairs. The filled oxygen p_{π} orbital of [OC₆F₅] is delocalized into the highly electron-withdrawing pentafluorophenyl ring which significantly reduces its ability for π -donation to the metal. Hence, the tantalum–oxygen p_{π} – d_{π} interactions are relatively weak and these bonds are intrinsically lengthened. This allows the dative π -bonding in the Ta(O₂)Ta bridge to be correspondingly strengthened. Meanwhile, the Cp* ligand is an extremely strong π -donor such that it dominates the competition for the Ta^V vacant d -orbitals; this is shown by the observations that the Ta—Cp* bonding is not distorted and the Ta—Cp*(centroid) distance [2.17 (3) Å] is short, as defined by its position within the lower quartile of all reported Ta—Cp*_{centroid} distances: LQ = 2.15 Å from a range of 2.05–2.53 (5) Å with $N = 412$ observations (Bruno *et al.*, 2002; CCDC, 1994). The Ta—CC_{aryl} bond length [2.20 (1) Å] has a fairly neutral contribution given its very typical length, *cf.* $\bar{x} = 2.23$ (4) Å from $N = 158$ observations.

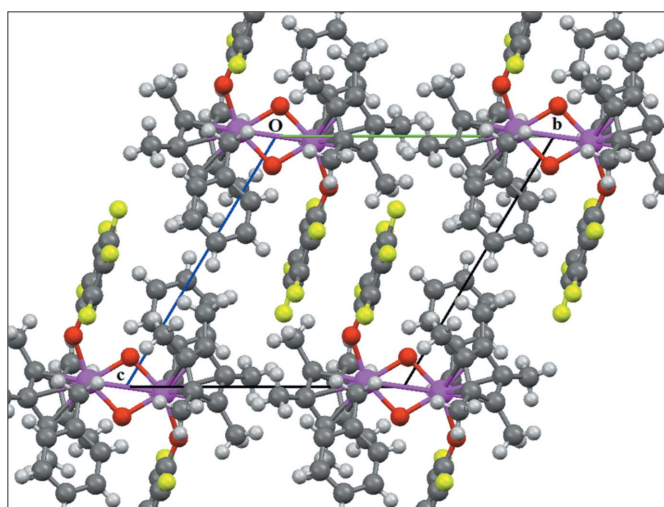
Aside from these electronic considerations, the structure of (4) displays severe steric congestion around each Ta atom; this appears to be alleviated by the twist angle of 77.1° between the

pentafluorophenyl ring (C1–C6) and the benzyl ring (C8–C13) (*see below*). The molecules pack with the Ta···Ta vectors aligned along the crystallographic b axis, while the pentafluorophenyl and benzyl groups lie in orthogonal orientations to each other, in the ac and bc planes, respectively; this enables good overlap between pentafluorophenyl rings (*see Fig. 5*) which are separated by 3.66 (1) Å. The pentafluorophenyl and benzyl rings are linked by a short non-bonded contact, F4···H10 A [2.61 (1) Å; symmetry code: $x, y, -1 + z$], while a weak contact pervades between the benzyl and cyclopentamethyl ring, C10···H16A [2.68 (1) Å; symmetry code: $-1 + x, y, z$].

3.2.2. Crystal structures of (5) and (6). Reaction of (2) with 2 equiv. of pentafluorophenol in n -heptane at 333 K results in the precipitation of yellow needle-shaped crystals. Their ¹H and ¹³C NMR spectra implies the loss of *t*-butylimido and neophyl groups while resonances for C₆F₅ units are observed in the ¹⁹F NMR spectrum. The nature of the crystals is confirmed to be Cp*Ta(OC₆F₅)₄ (5) by an X-ray crystal structure determination. The dimeric species [Cp*Ta(OC₆F₅)₂(μ -O)]₂ (6) is also isolated from the reaction mixture and structurally characterized.

Complex (5) is presumably generated by the reaction of (2) with four molecules of C₆F₅OH with the concomitant elimination of *t*-butylamine and two molecules of PhCMe₃. The mechanism for the formation of the μ -oxo dimer (6) is likely to be related to that for (4). Another possible pathway to (6) involves coupling of two molecules of (5) with the loss of C₆F₅OC₆F₅, but this is unlikely since the ratio of (5) and (6) in a benzene-*d*₆ solution did not alter over several months.

The crystal structure of (5) is shown in Fig. 6, and selected bond distances and angles are listed in Table 4. Fractional coordinates and anisotropic displacement parameters are given in the supplementary material.

**Figure 5**

Crystal packing diagram of (4) illustrating the Ta atoms projected along the crystallographic b axis, and the mutual orthogonality of the pentafluorophenyl and benzyl groups in the ac and bc planes: Ta (red), F (lime), C (dark grey), H (light grey). This figure is in colour in the electronic version of this paper.

Table 4

Selected bond lengths (Å) and angles (°) for (5).

Ta1—O1	1.985 (5)	O1—Ta1—O2	83.5 (2)
Ta1—O2	1.956 (8)	O1—Ta1—O3	85.6 (2)
Ta1—O3	1.907 (8)	O1—Ta1—Cp _{centroid}	104.0 (3)
Ta1—C1	2.43 (1)	O2—Ta1—O3	133.4 (3)
Ta1—C2	2.453 (8)	O2—Ta1—Cp _{centroid}	115.3 (3)
Ta1—C3	2.417 (7)	O3—Ta1—Cp _{centroid}	111.3 (3)
Ta1—Cp _{centroid}	2.111 (9)	Ta1—O1—C7	142.8 (5)
		Ta1—O2—C13	160.3 (7)
		Ta1—O3—C17	169.5 (7)

The molecule contains a mirror plane through O2 and O3 and the Ta atom resides in a distorted trigonal bipyramidal geometry. Rationale for the relatively long Ta—OC_{aryl} contacts [1.985 (5), 1.956 (8) and 1.907 (8) Å] has already been given [see discussion on (4), §3.2.1]. Adjacent pentafluorophenyl rings are approximately orthogonal [90.6 (9)°] to each other in (5), in the same way that the benzyl rings are near-orthogonal to the pentafluorophenyl rings in (4). This mutual ring orientation evidently minimizes the steric repulsion between the F atoms.

The crystal structure of (6) is shown in Fig. 7, and selected bond distances and angles are given in Table 5. Fractional coordinates and anisotropic displacement parameters are given in the supplementary material.

The molecule is a dimer with a highly distorted square-pyramidal arrangement around each Ta atom, but unlike the apparently related structure of (4) no inversion centre exists in (6). The largest Ta—O separation [2.014 (6) Å] exceeds that in (4) [2.005 (8) Å] and reflects the replacement of a benzyl group in (4) by an [OC₆F₅] group, which intensifies the competition between the π -donating ligands for the empty d_{π} metal orbitals. Meanwhile, the Ta1—O—Ta2 angles of 102.9 (3) and 103.8 (3)° are almost identical to that in (4) [103.3 (3)°].

Table 5

Selected bond lengths (Å) and angles (°) for (6).

Ta1—O1	1.973 (6)	O1—Ta1—O4	84.3 (3)
Ta1—O4	1.949 (6)	O1—Ta1—O10	83.3 (3)
Ta1—O10	1.972 (6)	O1—Ta1—O11	136.3 (3)
Ta1—O11	1.921 (6)	O1—Ta1—Cp _{centroid}	110.6 (5)
Ta1—C1	2.455 (8)	O4—Ta1—O10	140.8 (3)
Ta1—C2	2.480 (8)	O4—Ta1—O11	87.3 (3)
Ta1—C3	2.463 (9)	O4—Ta1—Cp _{centroid}	106.7(4)
Ta1—C4	2.424 (10)	O10—Ta1—O11	76.6 (2)
Ta1—C5	2.420 (9)	O10—Ta1—Cp _{centroid}	112.6 (4)
Ta1—Cp _{centroid}	2.13 (1)	O11—Ta1—Cp _{centroid}	113.0 (4)
Ta2—O2	1.937 (6)	O2—Ta2—O3	85.1 (3)
Ta2—O3	2.014 (6)	O2—Ta2—O10	129.1 (3)
Ta2—O10	1.934 (6)	O2—Ta2—O11	87.5 (3)
Ta2—O11	1.960 (6)	O2—Ta2—Cp _{centroid2}	110.3 (4)
Ta2—C30	2.431 (10)	O3—Ta2—O10	82.7 (2)
Ta2—C31	2.473 (11)	O3—Ta2—O11	146.1 (3)
Ta2—C32	2.463 (11)	O3—Ta2—Cp _{centroid2}	105.0 (4)
Ta2—C33	2.441 (11)	O10—Ta2—O11	76.6 (2)
Ta2—C34	2.381 (11)	O10—Ta2—Cp _{centroid2}	120.5 (4)
Ta2—Cp _{centroid2}	2.14 (1)	O11—Ta2—Cp _{centroid2}	108.5 (4)
		Ta1—O1—C6	145.4 (6)
		Ta2—O2—C12	162.8 (6)
		Ta2—O3—C18	134.5 (6)
		Ta1—O4—C24	168.6 (7)
		Ta1—O10—Ta2	102.9 (3)
		Ta1—O11—Ta2	103.8 (3)

Considering steric effects, the four relatively large aryloxide Ta—O—C_{ipso} angles range from 134.5 (6) to 168.6 (7)° and presumably contribute to a reduction in unfavourable repulsive forces between the pentafluorophenyl moieties. Consequently, the twist angles between the neighbouring pentafluorophenyl rings (range 34.1–57.3°; mean 42°) are markedly smaller than those in the benzyl/pentafluorophenyl analogue (4) (77.1°; Fig. 8). Compared with monomeric Cp*Ta(OC₆F₅)₄ (5), which exhibits large (OC₆F₅) twist angles

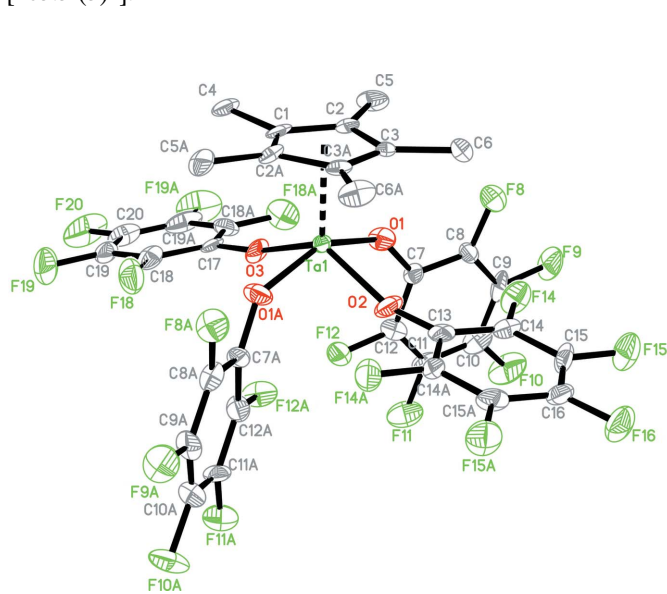


Figure 6

The molecular structure of (5) with anisotropic displacement parameters shown at the 50% probability level. H atoms have been omitted for clarity.

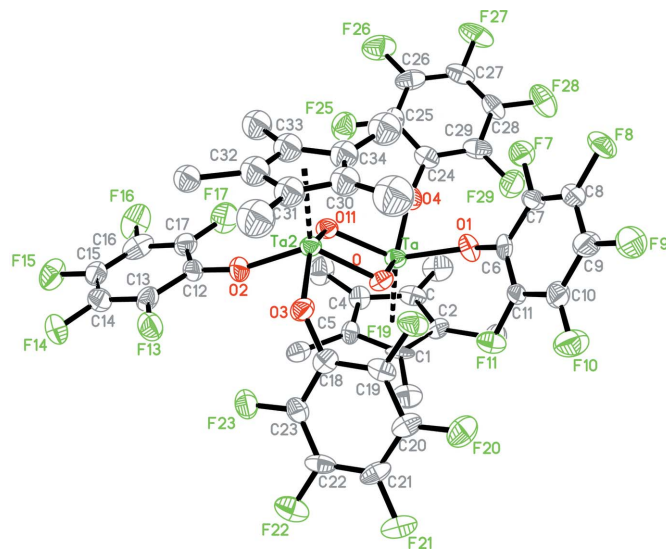


Figure 7

The molecular structure of (6) with anisotropic displacement parameters shown at the 50% probability level. H atoms have been omitted for clarity. The Cp* ring methyl groups are not labelled for reasons of clarity, but they can be inferred according to: (core Cp ring, label C*n*; methyl group, label C*n*A).

as previously discussed, the pentafluorophenyl rings in (6) experience less steric congestion due to the more undemanding nature of the dimeric geometry that is invoked by the oxo bridges. The extent of this twisting may also be influenced by intermolecular interactions. In particular, a short non-bonded contact, F15...F20 [2.89 (1) Å, symmetry code: $-1 + x, y, z$] rests between two pentafluorophenyl rings. Meanwhile, F9 and F10 are in close proximity to the disordered Cp* ring; the disorder renders difficult a quantification of interactions here, but H atoms encounter these F atoms at 2.37–2.55 (1) Å in this model.

Even at elevated temperatures in toluene, no reaction is observed between (3) and C₆F₅OH. This stability presumably results from the presence of α -agostic interactions. The stability may also have a steric origin: the Cp* and three bulky *t*-butyl groups form a virtual barrier to the inner coordination

sphere of the molecule (Fig. 2), thus preventing attack at the metal centre and imido moiety.

3.2.3. Concluding remarks. Six half-sandwich imido and aryloxo Cp*-tantalum complexes have been reported in this study. Therein, structure–reactivity relationships have been explored. In particular, the inertness of one imido Cp* tantalum complex (3) towards pentafluorophenol has been rationalized by the identification of α -agostic interactions. In contrast, the facile reaction of two imido Cp* tantalum complexes [(1) and (2)] with pentafluorophenol yields three aryloxo Cp*-tantalum compounds, whose crystal structures are dictated by competing steric and electronic interactions. The influential role of the pentafluorophenoxide ligand within the three different molecular environments of (4), (5) and (6) is shown to be particularly marked in this context.

The authors would like to thank the University of Durham for provision of all experimentation carried out in this study. JMC expresses her thanks to the Institut Laue–Langevin, Grenoble, France, and the EPSRC for financial support; the Royal Society for a University Research Fellowship; and the University of New Brunswick, Canada, for The Vice-Chancellor's Research Chair. MCWC wishes to thank the Research Grants Council of the Hong Kong SAR, China (CityU 100307), for financial support.

References

- Abbenhius, H. C. L., Feiken, N., Grove, D. M., Jastrzebski, J. T. B. H., Koojman, H., van der Sluis, P., Smeets, W. J. J., Spek, A. L. & van Koten, G. (1992). *J. Am. Chem. Soc.* **114**, 9773–9781.
- Abrahams, I., Bradley, D. C., Chudzynska, H., Motevalli, M. & O'Shaughnessy, P. (2000). *J. Chem. Soc. Dalton Trans.* pp. 2685–2691.
- Bell, A., Clegg, W., Dyer, P. W., Elsegood, M. J., Gibson, V. C. & Marshall, E. L. (1994). *J. Chem. Soc. Chem. Commun.* pp. 2547–2548.
- Brintzinger, H. H., Fisher, D., Mülhaupt, R., Rieger, B. & Waymouth, R. M. (1995). *Angew. Chem. Int. Ed. Engl.* **34**, 1143–1158.
- Bruno, I. J., Cole, J. C., Edgington, P. R., Kessler, M., Macrae, C. F., McCabe, P., Pearson, J. & Taylor, R. (2002). *Acta Cryst.* **B58**, 389–397.
- Buchwald, S. L. & Nielsen, R. B. (1988). *Chem. Rev.* **88**, 1047–1058.
- Buchwald, S. L., Watson, B. T. & Huffman, J. C. (1986). *J. Am. Chem. Soc.* **108**, 7411–7413.
- Buchwald, S. L., Watson, B. T., Wannamaker, M. W. & Dewan, J. C. (1989). *J. Am. Chem. Soc.* **111**, 4486–4494.
- Burckhardt, U., Casty, G. L., Gavenonis, J. & Tilley, T. D. (2002). *Organometallics*, **21**, 3108–3122.
- CCDC (1994). *Vista*. Cambridge Crystallographic Data Centre, 12 Union Road, Cambridge, UK.
- Chamberlain, L. R., Rothwell, I. P. & Huffman, J. C. (1986). *J. Chem. Soc. Chem. Commun.* pp. 1203–1206.
- Chien, J. C. W., Tsai, W. M. & Rausch, M. D. (1991). *J. Am. Chem. Soc.* **113**, 8570–8571.
- Coles, M. P., Dalby, C. I., Gibson, V. C., Clegg, W. & Elsegood, M. R. J. (1995). *J. Chem. Soc. Chem. Commun.* pp. 1709–1711.
- Ewen, J. A. & Elder, M. J. (1993). *Makromol. Chem. Macromol. Symp.* **66**, 179–190.
- Hlatky, G. C., Turner, H. W. & Eckman, R. R. (1989). *J. Am. Chem. Soc.* **111**, 2728–2729.
- Jordan, R. F. (1991). *Adv. Organomet. Chem.* **32**, 325–387.

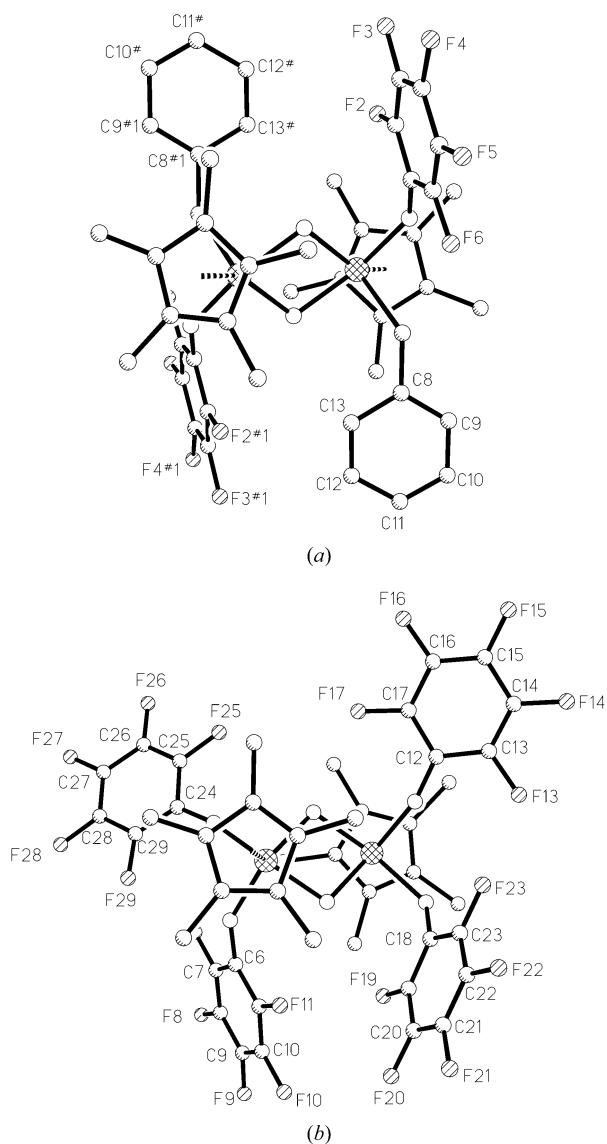


Figure 8

A comparison of twist angles between the benzyl/pentafluorophenyl rings in (4) (left; twist angle is 42°) and (6) (right; twist angle is 77.1°).

- Jordan, R. F., Bajgur, C. S., Willet, R. & Scott, B. (1986). *J. Am. Chem. Soc.* **108**, 7410–7411.
- Kaminsky, W. (1994). *Catal. Today*, **20**, 257–271.
- Kottke, T. & Stalke, D. (1993). *J. Appl. Cryst.* **26**, 615–619.
- Negishi, E. (1991). *Comprehensive Organic Synthesis*, edited by L. Paquette, Vol. 5, p. 1163. New York: Pergamon Press.
- Nugent, W. A. & Harlow, R. L. (1978). *J. Chem. Soc. Chem. Commun.* pp. 579–580.
- Nugent, W. A. & Mayer, J. M. (1988). *Metal–Ligand Multiple Bonds*. New York: Wiley Interscience.
- Poole, A. D., Williams, D. N., Kenwright, A. N., Gibson, V. C., Clegg, W., Hockless, D. C. R. & O’Neil, P. A. (1993). *Organometallics*, **12**, 2549–2555.
- Schmidt, S. & Sundermeyer, J. (1994). *J. Organomet. Chem.* **472**, 127–138.
- Schoettel, G., Kress, J. & Osborn, J. A. (1989). *J. Chem. Soc. Chem. Commun.* pp. 1062–1063.
- Schwartz, J. & Labinger, J. A. (1976). *Angew. Chem. Int. Ed. Engl.* **15**, 333–340.
- Sheldrick, G. M. (2008). *Acta Cryst.* **A64**, 112–122.
- Siemens Analytical X-ray Instruments (1994). *XSCANS*, Version 2.1. Siemens Analytical X-ray Instruments, Inc., Madison, Wisconsin, USA.
- Siemens Analytical X-ray Instruments (1995a). *SMART*, Version 4.050. Siemens Analytical X-ray Instruments, Inc., Madison, Wisconsin, USA.
- Siemens Analytical X-ray Instruments (1995b). *SAINTE*, Version 4.050. Siemens Analytical X-ray Instruments, Inc., Madison, Wisconsin, USA.
- Takahashi, T., Seki, T., Nitto, Y., Saburi, M., Rousset, C. J. & Negishi, E. (1991). *J. Am. Chem. Soc.* **113**, 6266–6268.
- Tidwell, J. H., Senn, D. R. & Buchwald, S. L. (1991). *J. Am. Chem. Soc.* **113**, 4685–4686.
- Tilley, T. D. (1993). *Acc. Chem. Res.* **26**, 22–29.
- Walker, N. & Stuart, D. (1983). *Acta Cryst.* **A39**, 158–166.
- Yang, X., Stern, C. L. & Marks, T. J. (1991). *J. Am. Chem. Soc.* **113**, 3623–3625.
- Yang, X., Stern, C. L. & Marks, T. J. (1994). *J. Am. Chem. Soc.* **116**, 10015–10031.